frontiers | Frontiers in Physics

TYPE Mini Review
PUBLISHED 12 October 2022
DOI 10.3389/fphy.2022.1013937

OPEN ACCESS

EDITED BY
Marcin Matusiak,
Institute of Physics, Polish Academy of Sciences, Poland

REVIEWED BY
Adrian Esteban Feiguin,
Northeastern University, United States
James Storey,
Victoria University of Wellington, New Zealand

*CORRESPONDENCE
Zhen-Su She,
she@pku.edu.cn

SPECIALTY SECTION
This article was submitted to Condensed Matter Physics, a section of the journal Frontiers in Physics

RECEIVED 08 August 2022
ACCEPTED 31 August 2022
PUBLISHED 12 October 2022

CITATION
Li R and She Z-S (2022), Energy-length scaling of critical phase fluctuations in the cuprate pseudogap phase. *Front. Phys.* 10:1013937. doi: 10.3389/fphy.2022.1013937

Energy-length scaling of critical phase fluctuations in the cuprate pseudogap phase

Rong Li and Zhen-Su She*

State Key Laboratory for Turbulence and Complex Systems, College of Engineering, Peking University, Beijing, China

The quantum origin of the cuprate pseudogap and its relationship to symmetry-breaking orders is a central conundrum of unconventional superconductors. The difficulty is deeply rooted in modeling simultaneous organizations in multiple degrees of freedom (including spin, momentum, and real space) generated by strong electron-electron correlations. Beyond early theories focusing on the description in spin and momentum space, recent studies turn to examine the spatial organization and intertwining mechanism of multiple orders. In this review, we summarize some progress in understanding the spatial organization of critical fluctuations and highlight the recent discovery of a universal energy-length scaling. This scaling quantitatively explains the nontrivial magnitude and doping dependence of the pseudogap energy and critical temperature and their relations to charge and superconducting ordering. We close with a prospect of the spatial organization mechanism of intertwined orders and its possible composite energy scaling.

KEYWORDS

pseudogap, spatial organization, critical fluctuations, energy-length scaling, doping dependence

1 Introduction

The origin of the pseudogap is one of the most critical problems for understanding the unconventional cuprate superconductivity [1–3]. This gap, Δ^*, features suppression of the electronic density of states around the Fermi level visible below a characteristic temperature T^* [4–7], see Figure 1A. In the momentum space, pseudogap is apparent only in the Brillouin zone's antinodal regions, where the d-wave superconducting gap reaches its maximum [8, 9], see Figure 1B. However, onset temperatures of the pseudogap and superconductivity show significantly distinct behaviors, i.e., T^* (as well as Δ^*) decreases linearly as doping (p) increases, while the superconducting transition temperature T_c (as well as the nodal gap) is dome-like [10, 11], see Figures 1A,C. This distinction is ubiquitous in hole-doped cuprates, indicating that the doping dependences of characteristic energies are critically related to the intrinsic nature of pseudogap.

Current theories about the pseudogap origin fall into four categories [2, 12], namely, a precursor of an ordered state (e.g., superconductivity [13–15] or spin density wave [16, 17]), a band folding gap induced by a (spin [18, 19] or charge [20, 21]) density wave order

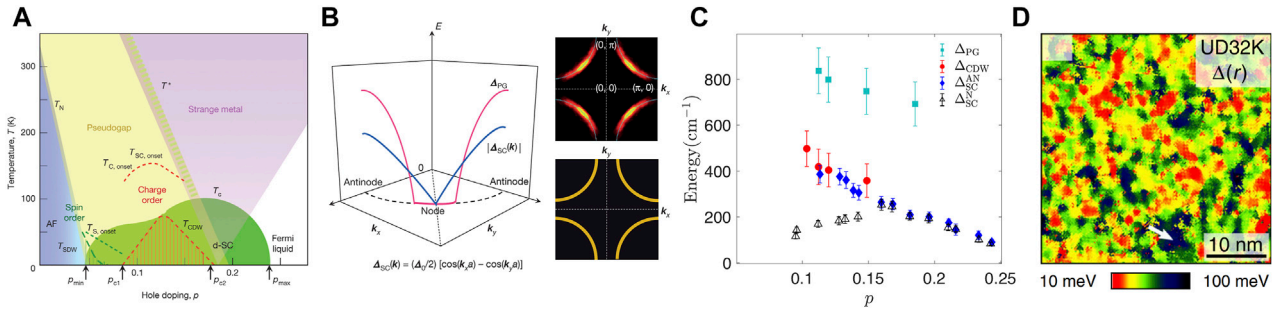

FIGURE 1
Pseudogap phenomena in cuprates. **(A)** The complex phase diagram for hole-doped cuprates [1], which shows the pseudogap phase and its associations with spin, charge, and superconducting orders. **(B)** Gap functions, Fermi arcs, and Fermi surface [1]. Once the pseudogap (Δ_{PG} in the left panel) sets in, the antinodal regions of the Fermi surface near the Brillouin zone edge are gapped out, giving rise to Fermi arcs (top right). **(C)** The doping dependencies of the pseudogap, the antinodal superconducting, and the CDW energy scales in $HgBa_2CuO_{4+\delta}$ with data from Ref. [11]. **(D)** The local spectral gap of an underdoped sample of $(Bi,Pb)_2(Sr,La)_2CuO_{6+\delta}$ measured by STM at each point, adapted from Ref. [42]. **(A)** and **(B)** are adapted from Ref. [1] with permissions.

(DWO), a hybrid gap induced by intertwined orders [22, 23] (e.g., stripe [24] and pair DWOs [25]), and a spectral feature from strong correlations (e.g., short-ranged magnetic fluctuations [26]) without breaking any symmetry. Although these theories have qualitatively described some pseudogap properties, none of them can precisely describe the whole pseudogap phase and all essential experimental manifestations; thus, there is no consensus on the pseudogap origin [2, 12, 26–28]. For instance, though the precursor to superconductivity could explain the T_c dome, its prediction of the T^* ends with the superconducting dome far beyond the experimentally observed critical doping p^* [2, 28]. On the other hand, numerical solutions of the Hubbard model obtain a correct T^* line, but it is hard to accurately determine the phase boundaries and the competition between density wave and uniform phases at a finite temperature [26]. Besides, intertwined orders involving both particle-particle (i.e., superconductivity) and particle-hole (e.g., DWO) pairing channels provide a comprehensive description of angle-resolved photoemission spectroscopy (ARPES) data [29, 30], but the stability of the emergent symmetry and the multiple wave vectors trick remains questionable [22, 31].

Therefore, thoroughly elucidating the pseudogap origin requires a unified description of multiple mechanisms to comprehensively describe the whole pseudogap phase and the main experimental manifestations [2, 22, 23]. However, this faces a fundamental difficulty rooted in the dual nature of cuprate electrons [12]. That is, the strong electron-electron correlations together with the chemical disorder generate simultaneous organizations in both momentum and spatial degrees of freedom, which have generally been treated separately as extended (or long-range) and local (or short-range) electronic states, respectively. Most previous theories [26, 30, 32–41] focus on the momentum side, e.g., particle-particle (or particle-hole) pairing with zero (or finite) total momentum, the umklapp scattering, to characterize the electronic dispersion and Fermi arcs. However, the spatial organization also results in nontrivial nanoscale inhomogeneity in the electronic structure, including nanoscale patterns of the gap energy scale (see Figure 1D), Fermi surface, and charge modulation in cuprates [42–50] observed by scanning tunneling microscope (STM). Owing to overlooking these nanoscale inhomogeneities, most momentum-resolved theories can only reach qualitative consistency with globally-averaged experimental observations but can not clarify the subtle local differences, which may be important to examine different mechanisms.

Studying the nontrivial organization mechanism in real space is crucial to breaking through this dilemma. Recently, accompanied by the observations of the nontrivial spatial pattern of charge ordering [46–52] and nematicity [53–56], theories focusing on spatial organization have been proposed for the vestigial nematicity [57], intertwined charge and superconductivity orders [58], and intertwined loop current and DWO [59]. These theories are mainly focused on specific intertwined mechanisms for distinct orders, which lack universality in describing the universal doping dependence of pseudogap energies (T^* and Δ^*). Therefore, it is crucial to discover a universal spatial organization mechanism that can yield quantitative descriptions for various cuprate compounds and orders. We note that the pseudogap phase contains a variety of mesoscopic orders, whose critical fluctuations affect the pseudogap phase. Furthermore, it is well known that critical fluctuations often have a universal scaling for various orders [60]. Therefore, this short review devotes to interpreting the recent finding of the universal energy-length scaling characterizing the spatial organization of local mesoscopic orders in the pseudogap phase. We will first derive this scaling, then show its application to charge density wave (CDW) and superconductivity, and close with a prospect about the spatial organization mechanism of intertwined orders.

2 Universal energy-length scaling associated with pseudogap phase

2.1 Universal scaling for critical phase fluctuations

In a real space perspective, the doping dependences of energy scales for the pseudogap [11, 61] correspond to varying spatial organizing structures of collective electron motions during the increase of hole spacing [62–64]. Therefore, the energy-length relation lies at the heart of the pseudogap origin and its relationship with symmetry-breaking orders [65]. It is well known that the strong electron-electron correlations stimulate multiple symmetry-breaking orders in cuprates, whose competitions result in unprecedented prominence of collective fluctuations [1]. These fluctuations are intimately related to and affect the pseudogap phase. For instance, the emergence of magnetic fluctuations [66, 67] and nematicity order coincide with the pseudogap opening temperature T^* [53–56], while the superconducting phase fluctuations defines T_c, the onset temperature of thermal vortices in the pseudogap phase [13, 68–70]. Therefore, we propose that the pseudogap phase can be treated as a "critical" phase (ansatz No. 1), which holds various quantum [63, 71–75] or thermal critical points and lines in the $T-p$ phase diagram. Thus, many collective fluctuations in this phase are of critical natures, e.g., having correlation functions with power law scalings. Although each order and its fluctuations have unique symmetry-broken form and energy, the common criticality may constrain the energy-length relationship to be a universal form.

In the following, taking pairing orders as an example, we derive this relation from the spatial organization of critical fluctuations. DWO and superconductivity are particle-hole and particle-particle pairings, respectively, with order parameters expressed by two-point correlation functions. In conventional metals, these orders are usually long-range coherent, so nontrivial pairing mainly occurs in the momentum space [76, 77]. On the contrary, strong electron-electron correlations and chemical disorder in cuprates constrain pairings to be short-range with coherence or correlation lengths at only several nanometers [20, 21, 78–80], revealing nontrivial spatial organizations [81–85]. Thus, we propose that they should be described by two-point correlation functions in real space. Moreover, for critical fluctuations, the universal criticality constrains the correlation function to be a power law versus length (ansatz No. 2), i.e., $g(l) \propto l^{-\eta}$, where η is a scaling exponent [60], l is the characteristic distance of pairing particle or hole.

In a classical theory of critical behavior, length scales are continuous coordinates. However, the Mott physics and strong correlations in cuprates result in a local tendency to phase separation [1], forcing the spatial organization of mesoscopic order and fluctuations occurring on specific nanoscales. Specifically, there are two kinds of length scales in the order parameter, i.e., the spatial period of the DWO and the characteristic length of the (charge, spin, or superfluid) density, presenting in phase and amplitude, respectively. Like Emery and Kivelson [13], we assume the critical fluctuations have the particle-wave duality constrained by the Heisenberg uncertainty principle (ansatz No. 3). Therefore, the energy scale corresponding to the two-point correlation function should satisfy an inverse square relation with its appropriate length as follows [65].

$$E_o = \gamma_o \frac{h^2}{m^* l_o^2}, \tag{1}$$

where E_o and l_o are the characteristic energy (e.g., gap and its onset temperature) and length (e.g., CDW period or Cooper-pair spacing) of a mesoscopic order, respectively, and m^* is the effective mass, h is the Planck constant, γ_o is a dimensionless parameter.

The scaling in Eq. 1 is universal for various phase-fluctuating orders. It can be derived from a series of physical mechanisms, including the phase-disordering transition (e.g., Berezinskii-Kosterlitz-Thouless (BKT) [86–88] and Bose-Einstein phase transition [89]), the umklapp scattering [65], and quantum kinetic energy of a density modulation[1]. For these mechanisms, γ_o is determined by a geometric factor, the amplitude and coupling strength, as well as the ratio between density fluctuations and mean-field, respectively. Different γ_o and l_o for various symmetry-breaking forms would yield different magnitude and doping dependence, providing quantitative criteria to determine dominant orders of the pseudogap, as shown in the following.

It is also intriguing to mention that the power law form of the energy-length scaling is universal for both quantum and classical systems. However, the scaling index may vary for different systems owing to different physical mechanisms. For instance, the gravity and electric potentials of a point source are inversely proportional to the distance to this point (−1 index), while the fluctuation energy called Reynolds stress of a turbulent flow is proportional to the square of the stress length (+2 index) [90]. In contrast, for simple quantum phenomena with only one related length scale, the inverse square scaling (−2 index) must be universal due to the dimensional constraints with Planck constant h (i.e., constant angular momentum).

2.2 Energy-period scaling of phase-fluctuating charge density wave

For the pseudogap origin, charge orders were identified as an important candidate in moderately doped cuprates. Recently, the

1 For a small ($\delta_\rho \ll \rho_0$) and unidirectional density modulation, the wave function can be expressed as $\psi(X) = \sqrt{\rho_0 + \delta\rho\cos(2\pi X/l_o)}$. The total quantum kinetic energy within a plaque with coherence lengths ξ_x and ξ_y can be obtained as $E_K = \int_s \psi^*(-\frac{h^2}{2m^*})\nabla^2\psi dXdy \approx \frac{(\delta\rho)^2\xi_x\xi_y}{16\rho_0}\frac{h^2}{m^* l_o^2}$.

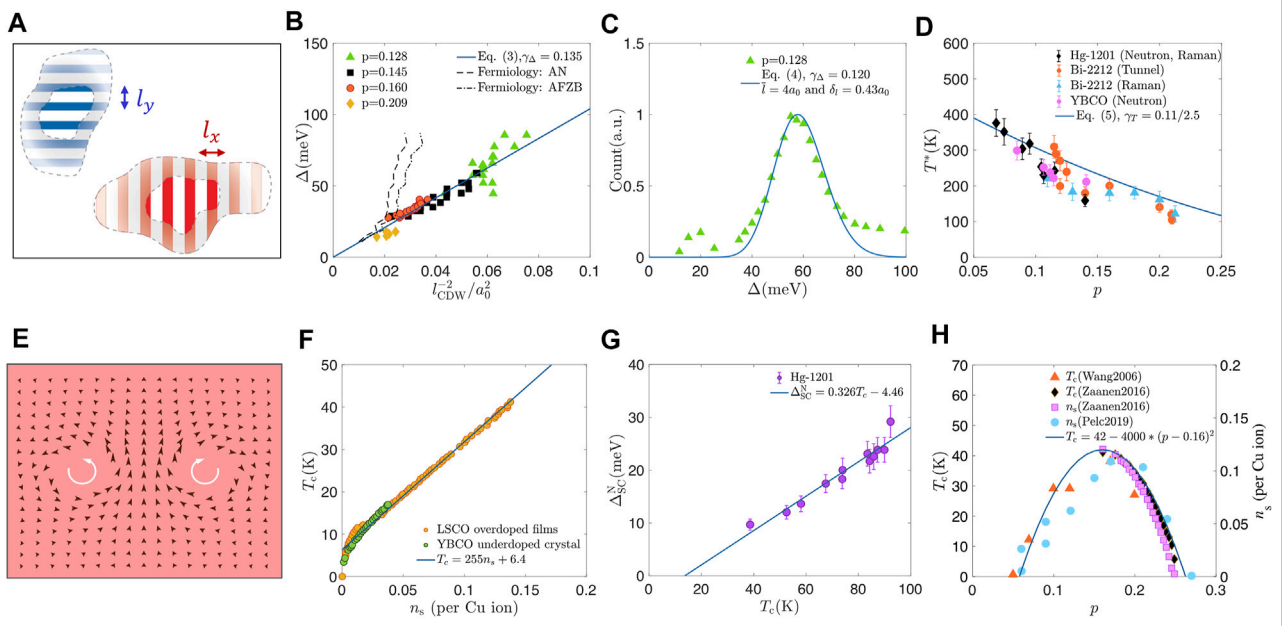

FIGURE 2
Universal spatial organization of mesoscopic orders and the energy-length scaling associated with pseudogap phase. **(A)** Schematic diagram of the locally unidirectional CDW along *x*- and *y*-axes [91]. **(B)** Scaling between the spectral gap and the CDW period. Symbols are data determined from the low-temperature (6 K) phase of Pb-Bi2201 samples [42], and the solid line is a prediction of Eq. 3. **(C)** Distributions of the spectral gap within the Pb-Bi2201 samples. Symbols are STM data from Ref. [42], and the solid line is a prediction from Eq. 4. **(D)** Doping dependence of the pseudogap onset temperature T^*. The symbols represent experimental data, and the solid line is a prediction from Eq. 5. **(E)** Unbinding of vortex-antivortex pairs, representing a spatial organization of the phase fluctuations. **(F)** The dependence of T_c on superfluidity at zero temperature [69]. **(G)** The linear dependence of the nodal superconducting gap Δ_{SC}^N on T_c. The data are determined from Ref. [11]. **(H)** The dome doping dependence of T_c and n_s. Symbols are experimental data determined from [92–94]. **(B)** and **(D)** are adapted from Ref. [65], and **(A)** and **(F)** are adapted from Refs. [69, 91] with permissions.

pseudogap opening at T^* was observed to coincide with the emergence of an electron-nematic order breaking the rotational symmetry [53–56], which is proposed to be generated by a partially melted unidirectional DWO with significant global phase fluctuations [8]. To test this assertion, it is crucial to quantify the spectral gap originating from a locally unidirectional CDW with space-time phase fluctuations. Taking the *x*-axis CDW in Figure 2A, for instance, this is considered as follows [65]:

$$\Psi(x,t) = A\exp[i(Q_o x + \phi(x,t))]. \tag{2}$$

Here, A is the amplitude of charge modulation, $Q_o = 2\pi/l_o$ is a phase-averaged wavevector, and $\phi(x,t)$ is the residual phase fluctuations, whose simplest expression is, for phason mode, $\phi(x,t) = qx - \omega_q t$. This fluctuating DWO generates an effective potential V proportional to the density wave modulations to induce the umklapp scattering (i.e., $\boldsymbol{k} \rightarrow \boldsymbol{k}' = \boldsymbol{k} + \boldsymbol{q} + n\boldsymbol{Q}_o$, where $\boldsymbol{k}$ and $\boldsymbol{k}'$ are the initial and final states, n is a nonzero integer). Following Lee and Rice [95], the characteristic energy of the mean scattering rate is $\Gamma = 4\pi m^* \sum |\boldsymbol{v}_k - \boldsymbol{v}_{k'}|^2 |\langle \boldsymbol{k}'|V|\boldsymbol{k}\rangle|^2 F_{\boldsymbol{k},\boldsymbol{k}'}$, where $\boldsymbol{v}_k$ and $\boldsymbol{v}_{k'}$ are velocity, $F_{\boldsymbol{k},\boldsymbol{k}'}$ is a complex function composed of Dirac and distribution functions. Under the assumption of small momentum difference ($\boldsymbol{v}_k - \boldsymbol{v}_{k'} \approx s\hbar(\boldsymbol{k} - \boldsymbol{k}')/m^*$) and long-wavelength approximation ($q \ll nQ_o$), we obtain $|\boldsymbol{v}_{k'} - \boldsymbol{v}_k|^2 \approx n^2 s^2 \hbar^2 Q_o^2/(m^*)^2$ [65]. Therefore, an energy gap related to umklapp scattering in the form of energy-period scaling is obtained as:

$$\Delta = \gamma_\Delta \frac{\hbar^2 Q_o^2}{m^*} = \gamma_\Delta \frac{h^2}{m^* l_o^2}, \tag{3}$$

which is a specific expression of Eq. 1.

Taking γ_Δ/m^* as constant for a moderate doping regime, Eq. 3 predicts an inverse square of energy-period scaling for cuprates, which is quantitatively consistent with the reported data of $(Bi,Pb)_2(Sr,La)_2CuO_{6+\delta}$ (Pb-Bi2201) [42], as shown in Figure 2B. In contrast, the previous theories [44, 96] attribute the connection between the pseudogap and Q_{CDW} to fermiology in momentum space, whose predictions show apparent overestimation for the optimal and underdoped regimes (see Figure 2B) due to the neglect of the renormalization of strong correlations [42, 96]. In contrast, the mean scattering strength $\gamma_\Delta = 0.135$ in our theory is found

to be close to the square ratio between the superexchange energy and the hopping energy ($J^2/t^2 \approx 0.11$ [42, 96]), revealing it is closely related to the antiferromagnetic correlation [22].

Another advantage of the energy-length scaling is its ability to characterize the global phase fluctuations, which was observed as spatial homogeneity of gap amplitude and period between different local CDW plaques. Assuming this phase fluctuations as a Gaussian type, we derive from Eq. 2 a gap distribution as [65]:

$$\Delta = f_0 \exp\left[-\frac{\left(\sqrt{\Delta} - \sqrt{\bar{\Delta}}\right)^2}{\left(\sqrt{\Delta_m} - \sqrt{\bar{\Delta}}\right)^2}\right], \tag{4}$$

where $\bar{\Delta} = \gamma_\Delta h^2/m^*\bar{l}^2$, $\Delta_m = \gamma_\Delta h^2/m^*(\bar{l} - \delta_l)^2$, $\bar{l}$ is the globally averaged value of l_{CDW}, δ_l is the standard deviation, and f_0 is the peak intensity. As shown in Figure 2C, the experimental observations are consistent with Eq. 4, indicating that both the local CDW and its global phase fluctuations satisfy the energy-length scaling.

Furthermore, the pseudogap opening temperature can be defined with the emergence of the particle-hole pairing of CDW [39], implying k_BT^* is proportional to the pseudogap energy [10, 11]. In other words, k_BT^* also satisfies the energy-length scaling as follows,

$$k_B T^* = \gamma_T \frac{h^2}{m^* l_o^2}. \tag{5}$$

As m^* are nearly constant in a moderate doping regime [97, 98], Eqs 3, 5 predict that the previously known monotonic decreases in T^* and Δ^* with increasing doping actually originates from the reduction of the CDW wavevector [20] and its amplitude [99]. As shown in Figure 2D and Ref. [65], this prediction is verified by experimental data of T^* and Δ^* over a wide doping range of various cuprate compounds [11, 100]. Therefore, the energy-length scaling provides solid proof that the pseudogap mainly originates from phase-fluctuating CDW in the moderate doping regime ($p = 0.1 \sim 0.2$). It is worth mentioning that the energy-length scaling may also be approximatively reflected in momentum-space structures, which is worth further exploration. For instance, we suspect that the antinodal pseudogap (3.5 or 2 times of local gap [65]) measured by ARPES or Raman response may have a similar inverse square relationship with the wave vector connecting the Fermi arc tips (close to the CDW wave vector [96]).

2.3 Energy-length scaling of superconducting phase fluctuations

Besides charge orders, superconducting phase fluctuations have been accepted as an important participator in part of the pseudogap regime [101]. It is well known that the two-dimensionality (2D) and low carrier density result in significant phase fluctuations in underdoped cuprates [13]. In the Berezinskii-Kosterlitz-Thouless (BKT) phase transition scenario [86, 88], the 2D superconducting phase fluctuations are generated by the real-space unbinding of vortex-antivortex pairs at a critical temperature, (see Figure 2E). The balance between the vortex excitation energy and the entropy (i.e., $E_\phi = T_cS_\phi$) determines this BKT phase transition temperature as [87]

$$k_B T_c = \frac{\pi\hbar^2 n_s}{2m^*} = \frac{\pi\hbar^2}{2m^* l_{cp}^2}, \tag{6}$$

where $l_{cp} = \sqrt{n_s}$ is the Cooper pair distance. Eq. 6 indicates that the phase coherence energy k_BT_c has an inverse square proportion to the Cooper-pair distance, satisfying the energy-length scaling Eq. 1. It provides another typical example of the energy-length scaling with length from the amplitude of a uniform phase but not the period of DWO.

Although there are other specific contexts to derive the scaling in Eq. 6 with different prefactors [13, 14], the linear scaling between T_c and n_s is now widely observed and accepted [68, 70]; see Figure 2F. Moreover, the recent observations of $\Delta_{SC}^N \propto T_c \propto n_s$ in both underdoped and overdoped cuprates [11, 68, 69] demonstrate that the superconducting dome of the nodal superconducting gap Δ_{SC}^N and T_c of thin cuprate films both originate from the dome-like doping dependence of the n_s, see Figures 2G,H. On the other hand, the relation between T_c and n_s in overdoped bulk samples shows more complexities [102] and need further clarifications. Furthermore, above the T_c dome, the BKT phase transition generates free thermal vortices in the low-T part ($T_c < T \ll T^*$) of the pseudogap phase. The best circumstantial evidence for this scenario comes from diamagnetism and Nernst signals [94, 103], which were accurately described by the time-dependent Ginzburg-Landau equation [104, 105] and vortex transport theory [106]. These evidences confirm that a spatial organization of superconducting phase-fluctuations (i.e., the unbinding of vortex-antivortex pair) determines the cuprate superconducting transition. However, contrary to Loktev et al.'s work [107] attributed the pseudogap formation mainly to superconducting phase fluctuations, we think the phase fluctuations of DWO dominate the upper pseudogap phase, and the superconducting phase fluctuations play a role in the pseudogap origin only in the lower part of the pseudogap phase.

It is intriguing that the present energy-length scaling (Eq. 1) also applies to the topological excitations of loop current in the strange metal phase at higher temperatures or beyond the pseudogap critical point [108]. These excitations are fluctuating vortices of unpaired electrons, whose characteristic

lengths are the thermal de Broglie wavelength ($l_T \propto T^{-1/2}$) or magnetic length ($l_B \propto B^{-1/2}$). These vortices scatter carriers with rates inversely proportional to the square of these lengths, which satisfies Eq. 1 and determines the well-known linear resistivity [108]. In summary, the above results in this section demonstrate the importance and universality of the spatial organization mechanism and the energy-length scaling for phase fluctuations of density wave, superconductivity, and loop current orders.

3 Outlook about the spatial organization and composite scaling of intertwined orders

Section 2 indicates that the pseudogap energies in the moderate doping regime are determined by the phase fluctuating CDW, and the thermally excited superconducting vortices survive in the low-T part of the pseudogap phase. Since these two kinds of order fluctuations coexist in a broad $T - p$ phase regime (Figure 1A), a natural question is whether the pseudogap arises from the intertwined orders of CDW with superconductivity. Indeed, many researchers believe that a thorough understanding of the pseudogap origin requires clarifying the intertwining relationship of multiple orders [22, 23]. Many experimental and theoretical studies have been carried out in this direction, introducing a novel spatially modulated superconducting phase [29, 30]. However, a universal spatial organization mechanism with quantitative description has not been present.

Here, we propose two critical open questions for the intertwined-order study from the spatial-organization perspective, i.e., what is the nanoscale pattern of intertwined orders in real space and how its composite energy-length scaling behaves. Recent STM and NMR measurements found that the CDW phase for underdoped cuprates [46–49] is locally unidirectional with significant global fluctuations, and the charge order can be locally enhanced in the superconducting vortex core [51, 52]. Thus, we believe there must be some nontrivial spatial organization pattern for intertwined orders of CDW, superconductivity, and loop-current order. For experiments, we suggest a combination of spatially resolved measurements to probe the spatial intertwining pattern of charge density, Cooper pair, and local magnetic excitation. More importantly, we suggest paying particular attention to examining the spatial distribution of topological excitations and orders (e.g., vortices and loop current), which may lie at the heart of intertwined mechanisms and the relationship between pseudogap and strange metal phases [67, 109]. For instance, we suspect that by increasing magnetic fields at low temperatures, superconducting vortices will likely emerge in the transition region between the x- and y-unidirectional CDWs (see Figure 2A) for energy optimization. Since introducing a vortex requires the emergence of a loop current with a varying velocity around a circle and a significant increase of kinetic energy, the transition region with varying wave vectors (contrast to the unidirectional region) and higher kinetic energy (than uniform region[1]) has both dynamical and thermodynamic advantages. Similarly, as the temperature rises close to T^*, we suspect the superconducting vortex may gradually transform into a loop current, resulting in many topological defects to drive the CDW into nematic order.

For theory, a critical question is whether intertwined orders have composite energy-length scalings, including characteristic lengths of different orders, or a simple scaling similar to Eq. 1. For example, there exist two anomalous energy scales: one is the antinodal superconducting gap Δ_{AC}^{SN} (defined by the peak signal of the B_{1g} Raman response below T_c [11]) with a monotonic decrease as the CDW gap (see Figure 1C); the other is the CDW onset temperature T_{CDW} with a dome dependence similar to the superconducting T_c (see Figure 1A), suggesting a possible intertwined mechanism between superconductivity and CDW. Do they come from composite energy scales, such as the product or quadrature coupling of two-order parameters [31, 51]? If so, does the scaling include characteristic lengths of CDW, superconductivity, or even loop current? We believe answers to these questions will help identify the origin of Δ_{AC}^{SN} and T_{CDW} and provide a quantitative criterion for advancing microscopic research of the intertwined orders.

4 Conclusion

The strong correlation and chemical disorder result in widespread nanoscale electronic structure in cuprates, making the spatial organization as crucial as the momentum-space organization. Exploring the spatial-organization mechanism of critical fluctuations, we find a simple scaling between the characteristic energy and length of mesoscopic order, which is universal to the phase fluctuations of CDW, superconductivity, and loop current. These results show that the spatial organization of critical fluctuations opens a new way to explore the relationship between the pseudogap and various order parameters and even the spatial organization of intertwined orders. Going forwards, we speculate that a comprehensive theory integrating the organizational principle in both real and momentum spaces is necessary to understand the pseudogap origins thoroughly in the future.

Author contributions

The manuscript was written by RL and ZS.

Funding

We acknowledge support from the National Natural Science Foundation of China with Grants Nos. 91952201 and 11452002.

Acknowledgments

We want to thank Lu-Hao Zhang, Zhen-Yuan Yin, and Yong Ji for their help preparing this manuscript.

Conflict of interest

The authors declare that the research was conducted in the absence of any commercial or financial relationships that could be construed as a potential conflict of interest.

Publisher's note

References

1. Keimer B, Kivelson SA, Norman MR, Uchida S, Zaanen J. From quantum matter to high-temperature superconductivity in copper oxides. *Nature* (2015) 518: 179–86. doi:10.1038/nature14165

2. Kordyuk AA. Pseudogap from ARPES experiment: Three gaps in cuprates and topological superconductivity (Review Article). *Low Temperature Phys* (2015) 41: 319–41. doi:10.1063/1.4919371

3. Hashimoto M, Vishik IM, He RH, Devereaux TP, Shen ZX. Energy gaps in high-transition-temperature cuprate superconductors. *Nat Phys* (2014) 10:483–95. doi:10.1038/nphys3009

4. Alloul H, Ohno T, Mendels P. ^{89}Y NMR evidence for a fermi-liquid behavior in $YBa_2Cu_3O_{6+x}$. *Phys Rev Lett* (1989) 63:1700–3. doi:10.1103/PhysRevLett.63.1700

5. Warren WW, Walstedt RE, Brennert GF, Cava RJ, Tycko R, Bell RF. Cu spin dynamics and superconducting precursor effects in planes above T_c in $YBa_2Cu_3O_{6.7}$. *Phys Rev Lett* (1989) 62:1193–6. doi:10.1103/PhysRevLett.62.1193

6. Homes CC, Timusk T, Liang R, Bonn DA, Hardy WN. Optical conductivity of c axis oriented $YBa_2Cu_3O_{6.70}$: Evidence for a pseudogap. *Phys Rev Lett* (1993) 71: 1645–8. doi:10.1103/PhysRevLett.71.1645

7. Loram JW, Luo J, Cooper J, Liang W, Tallon J. Evidence on the pseudogap and condensate from the electronic specific heat. *J Phys Chem Sol* (2001) 62:59–64. doi:10.1016/S0022-3697(00)00101-3

8. Ding H, Yokoya T, Campuzano JC, Takahashi T, Randeria M, Norman MR, Spectroscopic evidence for a pseudogap in the normal state of underdoped high-T_c superconductors. *Nature* (1996) 382:51–4. doi:10.1038/382051a0

9. Marshall DS, Dessau DS, Loeser AG, Park CH, Matsuura AY, Eckstein JN, Unconventional electronic structure Evolution with hole Doping in $Bi_2Sr_2CaCu_2O_{8+\delta}$: Angle-resolved photoemission results. *Phys Rev Lett* (1996) 76:4841–4. doi:10.1103/PhysRevLett.76.4841

10. Yoshida T, Malaeb W, Ideta S, Lu DH, Moor RG, Shen ZX, Coexistence of a pseudogap and a superconducting gap for the high-T_c superconductor $La_{2-x}Sr_xCuO_4$ studied by angle-resolved photoemission spectroscopy. *Phys Rev B* (2016) 93:014513. doi:10.1103/PhysRevB.93.014513

11. Loret B, Auvray N, Gu GD, Forget A, Colson D, Cazayous M, Universal relationship between the energy scales of the pseudogap phase, the superconducting state, and the charge-density-wave order in copper oxide superconductors. *Phys Rev B* (2020) 101:214520. doi:10.1103/PhysRevB.101.214520

12. Li T. A short review of the recent progresses in the study of the cuprate superconductivity. *Chin Phys B* (2021) 30:100508. doi:10.1088/1674-1056/abfa04

13. Emery VJ, Kivelson SA. Importance of phase fluctuations in superconductors with small superfluid density. *Nature* (1995) 374:434–7. doi:10.1038/374434a0

14. Lee PA, Nagaosa N, Wen XG. Doping a Mott insulator: Physics of high-temperature superconductivity. *Rev Mod Phys* (2006) 78:17–85. doi:10.1103/RevModPhys.78.17

15. Baskaran G, Zou Z, Anderson PW. The resonating valence bond state and high-T_c superconductivity — a mean field theory. *Solid State Commun* (1987) 63: 973–6. doi:10.1016/0038-1098(87)90642-9

16. Sedrakyan TA, Chubukov AV. Pseudogap in underdoped cuprates and spin-density-wave fluctuations. *Phys Rev B* (2010) 81:174536. doi:10.1103/PhysRevB.81.174536

17. Schmalian J, Pines D, Stojković B. Microscopic theory of weak pseudogap behavior in the underdoped cuprate superconductors: General theory and quasiparticle properties. *Phys Rev B* (1999) 60:667–86. doi:10.1103/PhysRevB.60.667

18. Yamada K, Lee CH, Kurahashi K, Wada J, Wakimoto S, Ueki S, Doping dependence of the spatially modulated dynamical spin correlations and the superconducting-transition temperature in $La_{2-x}Sr_xCuO_4$. *Phys Rev B* (1998) 57: 6165–72. doi:10.1103/PhysRevB.57.6165

19. Fujita M, Hiraka H, Matsuda M, Matsuura M, M. Tranquada J, Wakimoto S, Progress in neutron scattering Studies of spin Excitations in high-T_c cuprates. *J Phys Soc Jpn* (2012) 81:011007. doi:10.1143/jpsj.81.011007

20. Comin R, Damascelli A. Resonant X-ray scattering studies of charge order in cuprates. *Annu Rev Condens Matter Phys* (2016) 7:369–405. doi:10.1146/annurev-conmatphys-031115-011401

21. Frano A, Blanco-Canosa S, Keimer B, Birgeneau RJ. Charge ordering in superconducting copper oxides. *J Phys : Condens Matter* (2020) 32:374005. doi:10.1088/1361-648x/ab6140

22. Fradkin E, Kivelson SA, Tranquada JM. Colloquium: Theory of intertwined orders in high temperature superconductors. *Rev Mod Phys* (2015) 87:457–82. doi:10.1103/RevModPhys.87.457

23. Fernandes RM, Orth PP, Schmalian J. Intertwined vestigial order in quantum materials: Nematicity and beyond. *Annu Rev Condens Matter Phys* (2019) 10: 133–54. doi:10.1146/annurev-conmatphys-031218-013200

24. Tranquada JM, Sternlieb BJ, Axe JD, Nakamura Y, Uchida S. Evidence for stripe correlations of spins and holes in copper oxide superconductors. *Nature* (1995) 375:561–3. doi:10.1038/375561a0

25. Agterberg DF, Davis JS, Edkins SD, Fradkin E, Van Harlingen DJ, Kivelson SA, The physics of pair-density waves: Cuprate superconductors and beyond. *Annu Rev Condens Matter Phys* (2020) 11:231–70. doi:10.1146/annurev-conmatphys-031119-050711

26. Qin M, Schafer T, Andergassen S, Corboz P, Gull E. The Hubbard model: A computational perspective. *Annu Rev Condens Matter Phys* (2022) 13:275–302. doi:10.1146/annurev-conmatphys-090921-033948

27. Arovas DP, Berg E, Kivelson SA, Raghu S. The Hubbard model. *Annu Rev Condens Matter Phys* (2022) 13:239–74. doi:10.1146/annurev-conmatphys-031620-102024

28. Singh N. Leading theories of the cuprate superconductivity: A critique. *Physica C: Superconductivity its Appl* (2021) 580:1353782. doi:10.1016/j.physc.2020.1353782

29. He RH, Hashimoto M, Karapetyan H, Koralek JD, Hinton JP, Testaud JP, From a single-band metal to a high-temperature superconductor via two thermal phase transitions. *Science* (2011) 331:1579–83. doi:10.1126/science.1198415

30. Lee PA. Amperean pairing and the pseudogap phase of cuprate superconductors. *Phys Rev X* (2014) X4:031017. doi:10.1103/PhysRevX.4.031017

31. Pépin C, Chakraborty D, Grandadam M, Sarkar S. Fluctuations and the Higgs mechanism in underdoped cuprates. *Annu Rev Condens Matter Phys* (2020) 11: 301–23. doi:10.1146/annurev-conmatphys-031218-013125

32. Chakravarty S, Laughlin RB, Morr DK, Nayak C. Hidden order in the cuprates. *Phys Rev B* (2001) 63:094503. doi:10.1103/PhysRevB.63.094503

33. Li JX, Wu CQ, Lee DH. Checkerboard charge density wave and pseudogap of high-Tc cuprate. *Phys Rev B* (2006) 74:184515. doi:10.1103/PhysRevB.74.184515

34. Tremblay AMS, Kyung B, Sénéchal D. Pseudogap and high-temperature superconductivity from weak to strong coupling. Towards a quantitative theory (Review Article). *Low Temperature Phys* (2006) 32:424–51. doi:10.1063/1.2199446

35. Yang K-Y, Rice TM, Zhang F-C. Phenomenological theory of the pseudogap state. *Phys Rev B* (2006) 73:174501. doi:10.1103/PhysRevB.73.174501

36. Millis AJ, Norman MR. Antiphase stripe order as the origin of electron pockets observed in 1/8-hole-doped cuprates. *Phys Rev B* (2007) 76:220503. doi:10.1103/PhysRevB.76.220503

37. Norman MR, Kanigel A, Randeria M, Chatterjee U, Campuzano JC. Modeling the Fermi arc in underdoped cuprates. *Phys Rev B* (2007) 76:174501. doi:10.1103/PhysRevB.76.174501

38. Das T, Markiewicz RS, Bansil A. Competing order scenario of two-gap behavior in hole-doped cuprates. *Phys Rev B* (2008) 77:134516. doi:10.1103/PhysRevB.77.134516

39. Wang Y, Chubukov A. Charge-density-wave order with momentum (2Q, 0) and (0, 2Q) within the spin-fermion model: Continuous and discrete symmetry breaking, preemptive composite order, and relation to pseudogap in hole-doped cuprates. *Phys Rev B* (2014) 90:035149. doi:10.1103/PhysRevB.90.035149

40. Robinson NJ, Johnson PD, Rice TM, Tsvelik AM. Anomalies in the pseudogap phase of the cuprates: Competing ground states and the role of umklapp scattering. *Rep Prog Phys* (2019) 82:126501. doi:10.1088/1361-6633/ab31ed

41. Chakraborty D, Grandadam M, Hamidian MH, Davis JCS, Sidis Y, Pepin C. Fractionalized pair density wave in the pseudogap phase of cuprate superconductors. *Phys Rev B* (2019) 100:224511. doi:10.1103/PhysRevB.100.224511

42. Webb TA, Boyer MC, Yin Y, Chowdhury D, He Y, Kondo T, Density wave probes cuprate quantum phase transition. *Phys Rev X* (2019) X9:021021. doi:10.1103/PhysRevX.9.021021

43. Cai P, Ruan W, Peng Y, Ye C, Li X, Hao Z, Visualizing the evolution from the Mott insulator to a charge-ordered insulator in lightly doped cuprates. *Nat Phys* (2016) 12:1047–51. doi:10.1038/nphys3840

44. Wise WD, Chatterjee K, Boyer MC, Kondo T, Takeuchi T, Ikuta H, Imaging nanoscale Fermi-surface variations in an inhomogeneous superconductor. *Nat Phys* (2009) 5:213–6. doi:10.1038/nphys1197

45. Zeljkovic I, Xu Z, Wen J, Gu G, Markiewicz RS, Hoffman JE. Imaging the impact of single oxygen atoms on superconducting $Bi_{2+y}Sr_{2-y}CaCu_2O_{8+x}$. *Science* (2012) 337:320–3. doi:10.1126/science.1218648

46. Mesaros A, Fujita K, Edkins SD, Hamidian MH, Eisaki H, Uchida S, Commensurate $4a_0$-period charge density modulations throughout the $Bi_2Sr_2CaCu_2O_{8+x}$ pseudogap regime. *Proc Natl Acad Sci U S A* (2016) 113: 12661–6. doi:10.1073/pnas.1614247113

47. Zhang Y, Mesaros A, Fujita K, Edkins SD, Hamidian MH, Ch'ng K, Machine learning in electronic-quantum-matter imaging experiments. *Nature* (2019) 570: 484–90. doi:10.1038/s41586-019-1319-8

48. Zhao H, Ren Z, Rachmilowitz B, Schneeloch J, Zhong R, Gu G, Charge-stripe crystal phase in an insulating cuprate. *Nat Mater* (2019) 18:103–7. doi:10.1038/s41563-018-0243-x

49. Vinograd I, Zhou R, Hirata M, Wu T, Mayaffre H, Kramer S, Locally commensurate charge-density wave with three-unit-cell periodicity in $YBa_2Cu_3O_y$. *Nat Commun* (2021) 12:3274. doi:10.1038/s41467-021-23140-w

50. Wang X, Yuan Y, Xue QK, Li W. Charge ordering in high-temperature superconductors visualized by scanning tunneling microscopy. *J Phys : Condens Matter* (2019) 32:013002. doi:10.1088/1361-648x/ab41c5

51. Edkins SD, Kostin A, Fujita K, Mackenzie AP, Eisaki H, Uchida S, Magnetic field induced pair density wave state in the cuprate vortex halo. *Science* (2019) 364: 976–80. doi:10.1126/science.aat1773

52. Machida T, Kohsaka Y, Matsuoka K, Iwaya K, Hanaguri T, Tamegai T. Bipartite electronic superstructures in the vortex core of $Bi_2Sr_2CaCu_2O_{8+\delta}$. *Nat Commun* (2016) 7:11747. doi:10.1038/ncomms11747

53. Ishida K, Hosoi S, Teramoto Y, Usui T, Mizukami Y, Itaka K, Divergent nematic susceptibility near the pseudogap critical point in a cuprate superconductor. *J Phys Soc Jpn* (2020) 89:064707. doi:10.7566/JPSJ.89.064707

54. Sato Y, Kasahara S, Murayama H, Kasahara Y, Moon EG, Nishizaki T, Thermodynamic evidence for a nematic phase transition at the onset of the pseudogap in $YBa_2Cu_3O_y$. *Nat Phys* (2017) 13:1074–8. doi:10.1038/nphys4205

55. Murayama H, Sato Y, Kurihara R, Kasahara S, Mizukami Y, Kasahara Y, *Diagonal nematicity in the pseudogap phase of* $HgBa_2CuO_{4+\delta}$. *Nat Commun* (2019) 10:3282. doi:10.1038/s41467-019-11200-1

56. Wu J, Bollinger AT, He X, Bozovic I. Spontaneous breaking of rotational symmetry in copper oxide superconductors. *Nature* (2017) 547:432–5. doi:10.1038/nature23290

57. Nie L, Tarjus G, Kivelson SA. Quenched disorder and vestigial nematicity in the pseudogap regime of the cuprates. *Proc Natl Acad Sci U S A* (2014) 111:7980–5. doi:10.1073/pnas.1406019111

58. Hayward LE, Achkar AJ, Hawthorn DG, Melko RG, Sachdev S. Diamagnetism and density-wave order in the pseudogap regime of $YBa_2Cu_3O_{6+x}$. *Phys Rev B* (2014) 90:094515. doi:10.1103/PhysRevB.90.094515

59. Varma CM. Pseudogap and Fermi arcs in underdoped cuprates. *Phys Rev B* (2019) 99:224516. doi:10.1103/PhysRevB.99.224516

60. Pathria RK, Beale PD. *Statistical mechanics*. 3rd ed. Boston, MA, USA: Academic Press (2011).

61. Loret B, Auvray N, Gallais Y, Cazayous M, Forget A, Colson D, Intimate link between charge density wave, pseudogap and superconducting energy scales in cuprates. *Nat Phys* (2019) 15:771–5. doi:10.1038/s41567-019-0509-5

62. Komiya S, Chen HD, Zhang SC, Ando Y. Magic doping fractions for high-temperature superconductors. *Phys Rev Lett* (2005) 94:207004. doi:10.1103/PhysRevLett.94.207004

63. Proust C, Taillefer L. The remarkable underlying ground states of cuprate superconductors. *Annu Rev Condens Matter Phys* (2019) 10:409–29. doi:10.1146/annurev-conmatphys-031218-013210

64. Zhang H, Sato H. Universal relationship between T_c and the hole content in p-type cuprate superconductors. *Phys Rev Lett* (1993) 70:1697–9. doi:10.1103/PhysRevLett.70.1697

65. Li R, She Z-S. Unified energy law for fluctuating density wave orders in cuprate pseudogap phase. *Commun Phys* (2022) 5:13. doi:10.1038/s42005-021-00789-9

66. Zhang J, Ding Z, Tan C, Huang K, Bernal OO, Ho PC, Discovery of slow magnetic fluctuations and critical slowing down in the pseudogap phase of YBa_2 Cu_3O_y. *Sci Adv* (2018) 4:eaao5235. doi:10.1126/sciadv.aao5235

67. Varma CM. Colloquium: Linear in temperature resistivity and associated mysteries including high temperature superconductivity. *Rev Mod Phys* (2020) 92: 031001. doi:10.1103/RevModPhys.92.031001

68. Božović I, He X, Wu J, Bollinger AT. Dependence of the critical temperature in overdoped copper oxides on superfluid density. *Nature* (2016) 536:309–11. doi:10.1038/nature19061

69. Božović I, He X, Wu J, Bollinger AT. The vanishing superfluid density in cuprates—And why it matters. *J Supercond Nov Magn* (2018) 31:2683–90. doi:10.1007/s10948-018-4792-7

70. Uemura YJ, Luke GM, Sternlieb BJ, Brewer JH, Carolan JF, Hardy WN, Universal Correlations between T_c and n_s/m^* (carrier Density over effective mass) in high-T_c cuprate superconductors. *Phys Rev Lett* (1989) 62:2317–20. doi:10.1103/PhysRevLett.62.2317

71. Hussey NE, Buhot J, Licciardello S. A tale of two metals: Contrasting criticalities in the pnictides and hole-doped cuprates. *Rep Prog Phys* (2018) 81: 052501. doi:10.1088/1361-6633/aaa97c

72. Badoux S, Tabis W, Laliberte F, Grissonnanche G, Vignolle B, Vignolles D, Change of carrier density at the pseudogap critical point of a cuprate superconductor. *Nature* (2016) 531:210–4. doi:10.1038/nature16983

73. Fujita K, Kim CK, Lee I, Lee J, Hamidian MH, Firmo IA, Simultaneous transitions in cuprate momentum-space topology and electronic symmetry breaking. *Science* (2014) 344:612–6. doi:10.1126/science.1248783

74. Michon B, Girod C, Badoux S, Kacmarcik J, Ma Q, Dragomir M, Thermodynamic signatures of quantum criticality in cuprate superconductors. *Nature* (2019) 567:218–22. doi:10.1038/s41586-019-0932-x

75. Efetov KB, Meier H, Pépin C. Pseudogap state near a quantum critical point. *Nat Phys* (2013) 9:442–6. doi:10.1038/nphys2641

76. Bardeen J, Cooper LN, Schrieffer JR. Theory of superconductivity. *Phys Rev* (1957) 108:1175–204. doi:10.1103/physrev.108.1175

77. Monceau P. Electronic crystals: An experimental overview. *Adv Phys* (2012) 61:325–581. doi:10.1080/00018732.2012.719674

78. Wang Y, Ono S, Onose Y, Gu G, Ando Y, Tokura Y, Dependence of upper critical field and pairing strength on doping in cuprates. *Science* (2003) 299:86–9. doi:10.1126/science.1078422

79. Mourachkine A. Determination of the coherence length and the cooper-pair size in unconventional superconductors by tunneling spectroscopy. *J Supercond* (2004) 17:711–24. doi:10.1007/s10948-004-0831-7

80. Mukubwa A, Asselmeyer-Maluga T. Electron number density and coherence length of boson-fermion pair in HTSC. *Adv High Energ Phys* (2022) 2022:1–7. doi:10.1155/2022/8198401

81. Anderson PW, Lee PA, Randeria M, Rice TM, Trivedi N, Zhang FC. The physics behind high-temperature superconducting cuprates: The plain vanilla version of RVB. *J Phys : Condens Matter* (2004) 16:R755–69. doi:10.1088/0953-8984/16/24/r02

82. Zhang FC, Rice TM. Effective Hamiltonian for the superconducting Cu oxides. *Phys Rev B* (1988) 37:3759–61. doi:10.1103/physrevb.37.3759

83. Scalapino DJ. Superconductivity and spin fluctuations. *J Low Temp Phys* (1999) 117:179–88. doi:10.1023/A:1022559920049

84. Chen HD, Vafek O, Yazdani A, Zhang SC. Pair density wave in the pseudogap state of high temperature superconductors. *Phys Rev Lett* (2004) 93:187002. doi:10.1103/PhysRevLett.93.187002

85. Zhao JY, Two-hole ground state: Dichotomy in pairing symmetry. arXiv. AvaliableAt: https://arxiv.org/abs/2106.14898, (2021).

86. Berezinskii VL. Destruction of long-range order in one-dimensional and two-dimensional systems possessing a continuous symmetry group II. quantum systems. *Sov Phys JETP* (1972) 34 610.

87. Kosterlitz JM, Thouless DJ. Long range order and metastability in two dimensional solids and superfluids. (Application of dislocation theory). *J Phys C: Solid State Phys* (1972) 5:L124–6. doi:10.1088/0022-3719/5/11/002

88. Kosterlitz JM, Thouless DJ. Ordering, metastability and phase transitions in two-dimensional systems. *J Phys C: Solid State Phys* (1973) 6:1181–203. doi:10.1088/0022-3719/6/7/010

89. Pethick CJ, Smith H. *Bose–einstein condensation in dilute gases*. 2 ed. Cambridge, UK: Cambridge University Press (2008).

90. She Z-S, Chen X, Hussain F. Quantifying wall turbulence via a symmetry approach: A lie group theory. *J Fluid Mech* (2017) 827:322–56. doi:10.1017/jfm.2017.464

91. Comin R, Sutarto R, da Silva Neto EH, Chauviere L, Liang R, Hardy WN. Broken translational and rotational symmetry via charge stripe order in underdoped $YBa_2Cu_3O_{6+y}$. *Science* (2015) 347:1335–9. doi:10.1126/science.1258399

92. Wang Y, Li L, Ong NP. *Nernst effect in high-T_c superconductors*. *Phys Rev B* (2006) 73:024510. doi:10.1103/PhysRevB.73.024510

93. Zaanen J. Superconducting electrons go missing. *Nature* (2016) 536:282–3. doi:10.1038/536282a

94. Pelc D, Popcevic P, Pozek M, Greven M, Barisic N. Unusual behavior of cuprates explained by heterogeneous charge localization. *Sci Adv* (2019) 5:eaau4538. doi:10.1126/sciadv.aau4538

95. Lee PA, Rice TM. Electric field depinning of charge density waves. *Phys Rev B* (1979) 19:3970–80. doi:10.1103/PhysRevB.19.3970

96. Comin R, Frano A, Yee MM, Yoshida Y, Eisaki H, Schierle E. Charge order Driven by fermi-arc Instability in $Bi_2Sr_{2-x}La_xCuO_{6+\delta}$. *Science* (2014) 343:390–2. doi:10.1126/science.1242996

97. Padilla WJ, Lee YS, Dumm M, Blumberg G, Ono S, Segawa K, Constant effective mass across the phase diagram of high-T_c cuprates. *Phys Rev B* (2005) 72:060511. doi:10.1103/PhysRevB.72.060511

98. Dai YM, Xu B, Cheng P, Luo HQ, Wen HH, Qiu XG, Doping evolution of the optical scattering rate and effective mass of $Bi_2Sr_{2-x}La_xCuO_6$. *Phys Rev B* (2012) 85:092504. doi:10.1103/PhysRevB.85.092504

99. Peng YY, Fumagalli R, Ding Y, Minola M, Caprara S, Betto D, Re-entrant charge order in overdoped (Bi, Pb)$_{2.12}Sr_{1.88}CuO_{6+\delta}$ outside the pseudogap regime. *Nat Mater* (2018) 17:697–702. doi:10.1038/s41563-018-0108-3

100. He Y, Yin Y, Zech M, Soumyanarayanan A, Yee MM, Williams T, Fermi surface and pseudogap evolution in a cuprate superconductor. *Science* (2014) 344:608–11. doi:10.1126/science.1248221

101. Keimer B, Moore JE. The physics of quantum materials. *Nat Phys* (2017) 13:1045–55. doi:10.1038/nphys4302

102. Dordevic SV, Homes CC. Superfluid density in overdoped cuprates: Thin films versus bulk samples. *Phys Rev B* (2022) 105:214514. doi:10.1103/PhysRevB.105.214514

103. Li L, Wang Y, Komiya S, Ono S, Ando Y, Gu GD, Diamagnetism and Cooper pairing above T_c in cuprates. *Phys Rev B* (2010) 81:054510. doi:10.1103/PhysRevB.81.054510

104. Jiang X, Li D, Rosenstein B. Strong thermal fluctuations in cuprate superconductors in magnetic fields above T_c. *Phys Rev B* (2014) 89:064507. doi:10.1103/PhysRevB.89.064507

105. Mukerjee S, Huse DA. Nernst effect in the vortex-liquid regime of a type-II superconductor. *Phys Rev B* (2004) 70:014506. doi:10.1103/PhysRevB.70.014506

106. Li R, She ZS. A quantitative vortex-fluid description of Nernst effect in Bi-based cuprate high-temperature superconductors. *New J Phys* (2017) 19:113028. doi:10.1088/1367-2630/aa8cee

107. Loktev VM, Quick RM, Sharapov SG. Phase fluctuations and pseudogap phenomena. *Phys Rep* (2001) 349:1–123. doi:10.1016/S0370-1573(00)00114-9

108. Li R, She ZS. Emergent mesoscopic quantum vortex and Planckian dissipation in the strange metal phase. *New J Phys* (2021) 23:043050. doi:10.1088/1367-2630/abeeba

109. Giustino F, Lee JH, Trier F, Bibes M, Winter SM, Valenti R, The 2021 quantum materials roadmap. *J Phys Mater* (2020) 3:042006. doi:10.1088/2515-7639/abb74e